Architecture-Scale Human-Assisted Additive Manufacturing

Hironori Yoshida[1]*, Takeo Igarashi[1], Yusuke Obuchi[1], Yosuke Takami[1], Jun Sato[1], Mika Araki[1], Masaaki Miki[1], Kosuke Nagata[1], Kazuhide Sakai[2], and Syunsuke Igarashi[2]

[1]The University of Tokyo [2]Shimizu Corporation

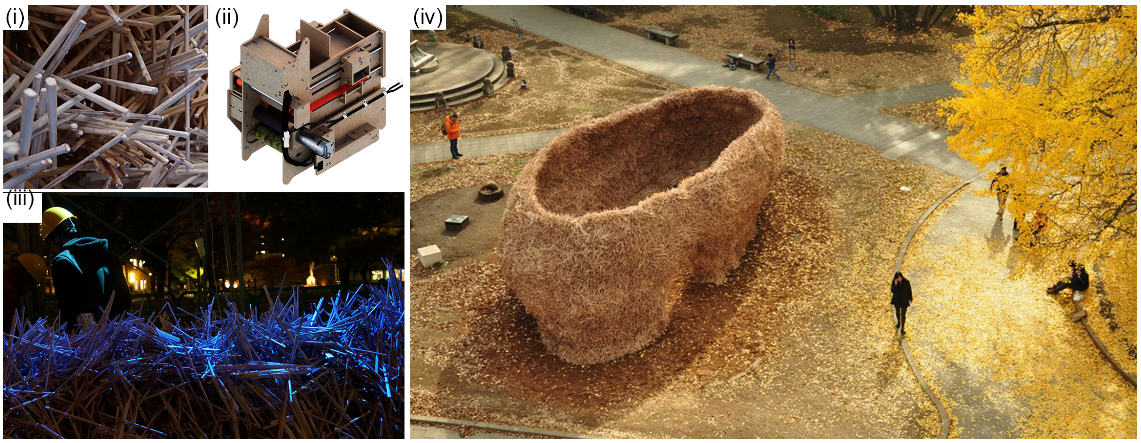

Figure 1: *An overview of our method: (i) aggregation of printed chopsticks solidified with wood glue; (ii) a specially developed handheld printing device to consistently feed a chopstick-glue composite; (iii) print guidance system implemented by a projector-camera system; (iv) the constructed pavilion as a case study. Note that the method is still experimental, and the upper part of this pavilion was constructed separately as panels and assembled later.*

Abstract

Recent digital fabrication tools have opened up accessibility to personalized rapid prototyping; however, such tools are limited to product-scale objects. The materials currently available for use in 3D printing are too fine for large-scale objects, and CNC gantry sizes limit the scope of printable objects. In this paper, we propose a new method for printing architecture-scale objects. Our proposal includes three developments: (i) a construction material consisting of chopsticks and glue, (ii) a handheld chopstick dispenser, and (iii) a printing guidance system that uses projection mapping. The proposed chopstickglue material is cost effective, environmentally sustainable, and can be printed more quickly than conventional materials. The developed handheld dispenser enables consistent feeding of the chopstickglue material composite. The printing guidance system — consisting of a depth camera and a projector — evaluates a given shape in real time and indicates where humans should deposit chopsticks by projecting a simple color code onto the form under construction. Given the mechanical specifications of the stickglue composite, an experimental pavilion was designed as a case study of the proposed method and built without scaffoldings and formworks. The case study also revealed several fundamental limitations, such as the projector does not work in daylight, which requires future investigations.

CR Categories: I.3.6 [Computer Graphics]: Methodology and Techniques—Interaction Techniques I.3.5 [Computer Graphics]: Computational Geometry and Object Modeling—Physically based modeling;

Keywords: 3D printing, Fabrication

1 Introduction

Digital fabrication has become more prevalent in recent years due to the increased accessibility of a range of personal digital fabrication tools. In the architectural domain, such tools have been in use for years in both professional practices and educational settings. However, unlike CAD software (which fully replaced conventional drafters), applications of these tools are limited either to custom component fabrication or scale model making. Additionally, these digital fabrication tools can never fully replace the role of humans in construction and development processes. Human labor is still essential when dealing with uncertainties in on-site construction processes because humans are able to flexibly determine case-by-case solutions. This is primarily due to the one-off nature of architectural design. Moreover, digital fabrication tools were originally designed for factory automation in controlled environments, thus not immediately applicable to construction sites [Bock 2007].

There have been some attempts to scale up 3D printer to building scale; however, a massive CNC gantry base has been an issue to be resolved and available materials are limited. The D-shape has a

*e-mail:hironoriyh@gmail.com

large print head with 300 array injection nozzles (6 X 6 m model), solidifying sand layers at 1.0 mm resolution [Cesaretti et al. 2014]. Contour Crafting developed a nozzle for cement extrusion and controlled it with a large CNC gantry [Khoshnevis 2004], and a Chinese company Yingchuang (WinSun) applied it to actual building construction [Frearson 2014]. DUS Architecten developed a relatively large printer in collaboration with Ultimaker for a canal house project [Bogue 2013].

Our proposal for scaling up 3D printing mechanisms was inspired by recent works related to computer-assisted digital fabrication processes [Zoran et al. 2013; Rivers et al. 2012b],especially ShapeShift and Sculpting by Numbers, which make it easy to sculpt clay by projecting simple colors on a work [Skeels and Rehg 2007; Rivers et al. 2012a]. This process is applicable to additive manufacturing, wherein workers hold a printing nozzle and are told where to print. Because one of the primary challenges for large-scale printing is the determination of a material solution, a related challenge is the development of a handheld printing nozzle and a corresponding guidance system.

In this paper, we present an architecture-scale, computer-assisted digital fabrication method consisting of three technical components: (i) a porous printing material composite consisting of chopsticks and wood glue, (ii) a specially designed printing device called a "stick dispenser," and (iii) a printing guidance system. For large-scale 3D printing purposes, the simple, straight geometry of chopsticks has advantages in terms of efficiency, production, and logistics. Chopsticks and wood glue are dropped together, forming randomly aggregated porous structures that are evaluated through volume-based analyses. The mechanical specifications of aggregated chopsticks are obtained through material tests, and these specifications are then used to inform the subsequent pavilions design process. To ensure a consistent feed of the stickglue composite, the dispenser was created to be capable of controlling the aggregation process. The projectorcamera system was developed to evaluate shapes in real time and then indicate to human workers where to print, all through the use of a simple color code. The system enables the materialization of digital models with minimal use of fabrication equipment.

With the developed method, we designed an experimental pavilion as a case study (50 m^2 footprint and 3.8 m height) and constructed it without large scaffoldings and redundant formworks. Due to the time constraints and daylight issue of operating a projector, only part of the pavilion (up to 1 m) was printed on-site; the rest was assembled with prefabricated panels (further discussed in Section 7). In spite of these limitations, we believe the individual components of this work advance state-of-the-art architecture regarding design and fabrication. Furthermore, the method as a whole—including the construction process—provides insights and inspirations for future advancements in architecture-scale digital fabrication.

2 Related Works

Recently, many works using 3D printers have focused both on creating objects and enhancing their properties (e.g., strength, movability, and deformability). Many papers have proposed 3D printing methods that analyze an input 3D model and create a structurally durable model [Zhou et al. 2013; Lu et al. 2014]. Pereira et al. [2014] focused on propagation of light inside a solid object and proposed a manufacturing method that prints an object with embedded optical fibers that route light between two surfaces. Prevost et al. [2013] proposed a method of assisting users in producing properly balanced designs for 3D printing designs so that printed models can stand without supports. Cali et al. [2012] proposed a method of printing objects with movable mechanical joints. To measure deformations of non-linear materials, some previous works have proposed a capture-and-model method for nonlinear heterogeneous soft tissue [Bickel et al. 2009; Pai et al. 2001]. These studies mainly discuss methods of capturing the deformations of a real object and modeling those deformations as finite-element models [Bickel et al. 2010].

Architectural design has been taking advantage of computer graphics [Dorsey and McMillan 1998]. Recent works have focused on masonry structures to make self-supported structures [Whiting et al. 2012; De Goes et al. 2013; Vouga et al. 2012]. Panozzo et al. [2013] proposed a method that allows end users to create free-form, self-supported masonry structures; Deuss et al. [2014] then optimized the construction process by reducing the number of supports. Song et al. [2013] described an interactive computational tool for designing a reciprocal frame structure. These works proposed novel modeling methods within the constraints of conventional construction processes and materials; however, none address a drastic change in building materials nor have they been validated by constructing large-scale objects. A bottom-up approach (such as initiating a change in building materials) will eventually affect construction and modeling methods. For example, Dierichs et al. [2010] aggregated a large quantity of spike-shaped elements and presented the resulting forms, but they were limited to small-scale prototypes and did not demonstrate a novel approach to computational design. As a large-scale aggregation, Quinze randomly connected 2 X 4 timber planks and exhibited a pavilion at the Burning Man festival [Fairs 2002]. These studies employed aggregation as an approach to form finding, but not as a construction method augmented by computational assistance.

Projection-based augmented reality has been used for various purposes (e.g., for tangible displays, entertainment, and task guidance), and many works have advanced its performance [Azuma et al. 1997; Raskar et al. 1998; Piper et al. 2002]. These works primarily employed projector-camera systems because configurations consisting of a projector and a camera are simple and easy to set up with an interactive system without having to wear any equipment. MirageTable is an interactive system that captures objects and provides 3D visualizations with shutter glasses [Benko et al. 2012]. Some other works use projector-camera systems to augment the surfaces of entire rooms [Wilson et al. 2012; Jones et al. 2014; Benko et al. 2014]. Because the projector-camera system is an interactive system, it is effective for use in a task guidance context. Flagg et al. [2006] used the projector-camera system to guide painting, employing it as traditional media and as a tool for non-expert users. Origami Desk [2002] is a guiding system for origami that projects the flow of origami construction. Sodhi et al. [2012] projected the guidance directly onto a user to indicate the desired motions.

In consideration of these works, this paper begins presentation of the conducted research with an examination of the properties of the proposed material. The proposed material is used in conjunction with computational assistance to construct an architecture-scale object.

3 Material

We choose the combination of chopsticks (Japanese ceder) and glue (Konishi CHR-55) as a construction material for the following reasons; First, it forms a highly porous structure. A porous structure is desirable because one can produce a large structure out of less material, resulting in shorter operation time. Secondly, the straight shape has advantages in production and logistics. Finally and most importantly, chopsticks are cheap and easily obtainable. Each stick costs less than a dollar, and in China alone, more than 80 billion chopsticks are produced annually. Costs and environmental impacts can be further reduced by using imperfect chopsticks (chopsticks resulting from errors in the manufacturing process).

This section includes a report on our study of the proposed material for design and construction purposes. After making a number of test samples with a dispenser (Section 4), we empirically studied the form-ability and the constraints of aggregated sticks, referring to them as "geometric properties". Testing these samples through compression and bending tests, we obtained mechanical properties of sticks per volume. We eventually used these geometric and mechanical properties to design the pavilion and simulate its structural capabilities (see Section 6).

3.1 Geometric Properties

This section examines form-ability of stick aggregation and its limitations. The stick geometry contributed to quick printing operation; for example, chopsticks with 220 mm length can add 100-200 mm per layer, depending on the rotation of the sticks at the point from which they are dropped. Stick aggregation can grow not only vertically (see Figure 2 (i)) but also obliquely upward without any support underneath by changing the dropping angle. A 60 cm overhang could be built at 150 cm height, as Figure 2 (iii) illustrates. The overhang without formworks is a strong advantage for construction.

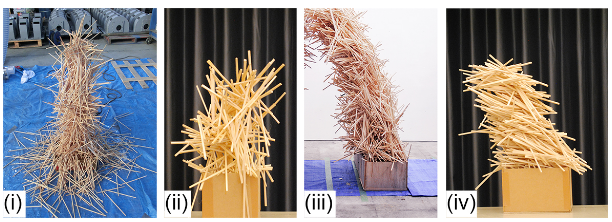

Figure 2: *Geometric properties: A vertically printed sample (i) with jammed structure (ii). An obliquely printed sample (iii) with stratified structure (iv).*

Mode of Aaggregation:
We distinguished two modes of aggregation: jammed and stratified (see Figure 2(ii) and (iv), respectively), determined by the angle at which sticks were dropped (see Table 1). When sticks were dropped vertically, the sticks landed in random locations and formed a jammed aggregation. To create a porous and lightweight structure, this process results in quick aggregation; thus, we usually print in jammed aggregation. For oblique growth, sticks need to be dropped at a certain angle and slower speed. This forms a stratified aggregation with layers of aligned sticks (see Figure 2). We built an oblique wall by carefully stratified aggregation and then dropped sticks in a jammed manner. In this way, the oblique wall worked as a formwork.

Table 1: *Input factors and resulting geometry*

Factors of control	Aggregation mode	Growth direction
Tilted dropping angle, spiked geometry at landing point	Jammed	Straight
Straight dropping angle, flat geometry at landing point	Stratified	Oblique

Factors of Control:
Among a range of factors of control, dropping angle, and speed influence the aggregation mode, as previously explained (illustrated in Section 4, Figure 7). Stratified aggregations require slower speeds for accurate deposition, whereas vertical dropping can be accomplished at higher speeds. However, to prevent sticks from bouncing at the landing point, the speed at the drop point can not be too fast. For the same reason, the drop point must be raised as the aggregation grows; this maintains a constant distance between the drop point and the landing point.

In addition to control parameters at the drop point, the initial geometry at the landing point also influences the aggregation mode. Dropping sticks onto a flat surface results in a flat, dense aggregation, whereas dropping onto a non-flat surface results in a jammed, porous structure. In our experiments, we prepared a container to initiate jammed aggregation (Figure 2 (ii) - (iv)). Table 2 summarizes major factors of control during dropping sticks.

Table 2: *Input factors explored in sample fabrication*

	Factors	Parameters
Factors when sticks are dropped	Dropping angle	0 (vertical) to 45 degree
	Dropping speed	Slow <->High
	Dropping height	Fixed <->Variant height
External factors	Glue drying speed	Fast (liquid-like) <->Slow (Sticky)
	Landing point geometry	Spiked <->Flat

3.2 Mechanical Properties

During structural analyses, the material was not modeled with aggregations of sticks. Instead, homogeneous volumes were used. Mechanical properties were acquired through a variety of loading tests performed on aggregated sticks. Seven samples were prepared and varied in the number of sticks and the amount of glue per volume. These samples were used for compression and 3-point bending tests (Figure 3). Figures 4 and 5 show the results of the compression and bending tests, respectively.

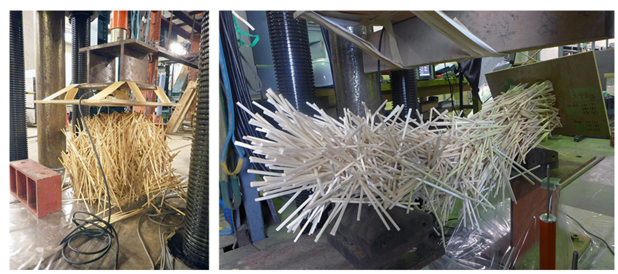

Figure 3: *Material tests: Compression test (left) with a 40 x 40 x 30 cm sample. A 3-points bending test (right) with a 25 x 27 x100 cm sample. A capping plate was placed without cutting the samples.*

We set a required density for constructing the pavilion to be $\rho = 0.06(\mathrm{tf}/\mathrm{m}^3)$, considering the average density of samples and safety margins. To achieve this density, 33,000 chopsticks and 33 (kg) wood glue were consumed per cubic meter. During material tests, the material and the testing device were not tightly connected, so there was a slippage at the beginning in some cases; in those instances, we calculated its Young's modulus starting from the point where the slippage stopped (Figure 4 and 5). After the treatment, all samples showed relatively similar values for yielding points and Young's modulus. We set the material's yielding point and Young's modulus after considering the averaged values and margin of safety. After treatment, all samples showed relatively similar values point and Young's modulus. Table 3 compares the mechanical specifications of stick aggregations with different materials. The data indicates that the material is quite weak, but it is also lighter than standard materials. The material exhibiting properties most similar to

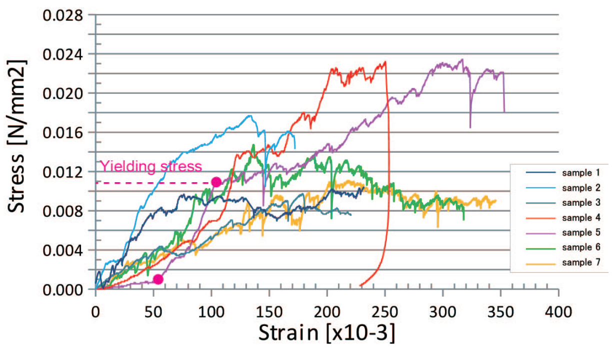

Figure 4: *Stress-strain curves from compression tests. Sample No. 5 showed that the load was slipping at the beginning.*

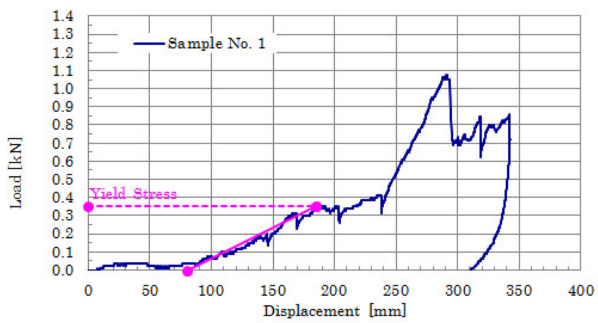

Figure 5: *A bending load-deformation curve from a 3-points bending test.*

the aggregated stick material is styrene foam [Lovatt and Shercliff 2002].

Table 3: *Comparison of mechanical specifications of stick aggregation and other materials.*

	Density (t/m^3)	Young's modulus (MPa)	Yield stress (MPa)
Stick aggregation	0.060	0.1	0.0106
Styrene foam	0.013	8	0.1
Balsa wood(across the grain)	0.140	150	1
Balsa wood(with the grain)	0.140	4000	10
Ceder wood(with the grain)	0.380	8000	25
Steel(SS400)	7.800	205000	400

The bending test demonstrated material strength greater than the strength observed in the compression tests. The sticks themselves have an anisotropic nature due to their geometry, thus producing differentiations in mechanical properties in accordance with differentiations in the direction of applied force. Furthermore, the direction of the applied force determined the amount of friction on the jammed structure. The results suggest that the material is capable of withstanding bending forces. These findings informed the design of the pavilion (see Section 6) and imply that a uniform surface (such as a shell) could be compatible with the material properties.

4 Stick Dispenser

After creating a series of prototypes, we arrived at the design of a hand-held stick dispenser, a machine capable of consistently depositing the stick-glue composite (Figure 6). There were three key design criteria for the dispenser: (1) capable of consistent material deposition when combining stick and glue feeding processes together, (2) ease in handling (regarding its size and weight), and (3) capable of controlling both dropping angle and speed for free-form construction (Section 3).

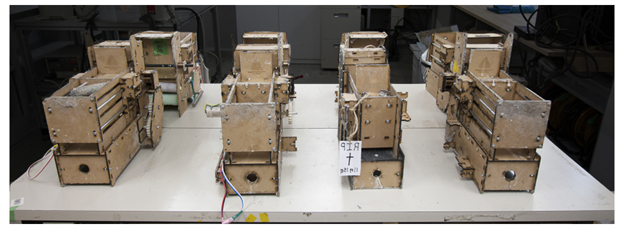

Figure 6: *A series of hand-held dispensers.*

Material Supply and Feeding Mechanism
A bundle of 300 sticks was supplied to a sliding container on the dispenser, which pushed sticks against a feed roller for feeding at any angle (Figure 7). The feed roller fed 10 sticks at a time through a slit, and then passed the sticks to glue coaters, evenly coating the sticks with wood glue. Both feeding and coating the rollers were powered by a DC motor with variable speed control. When considering the wood glue, it was important to determine the viscosity of glue, factor in the pumping pressure required, friction encountered within the hose, and glue drying speed. In particular, glue drying speed affects the aggregation mode (as described in Section 3). Thicker glue dries faster and thus holds the sticks where they are dropped; this makes it difficult to control the dropping angle. Thinner glue takes more time to dry (and thus holding the sticks in place), but it allows precise control in terms of dropping angle and speed. Our results indicated the optimum glue viscosity is 2.0 $Pa \cdot s$, with water and glue being mixed at a ratio of $1 : 3.25$, respectively. A gear pump with 3.0 MPa pressure can feed the glue.

Operation
During operation, users need to adjust the height of the dispenser in order to keep a constant distance between the dispenser and the top of the current work. A dispenser can feed 150 sticks and 1 liter of glue per minute (capable of printing 1 cubic meter in 1.5 hours). In oblique growth, users need to adjust the rotation of the dispenser in order to follow the growth direction. Through the use of a guidance system (Section 5), users can check the growth direction. Multiple dispensers can be operated within the guidance system.

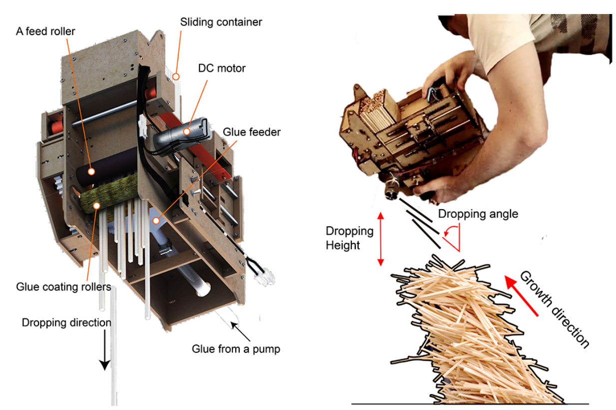

Figure 7: *Left: dispenser overview. Right: dispenser operation.*

Logistics for Large Quantities of Sticks
Although bundles of sticks were supplied manually with the hand-held dispenser, we also tested a logistical solution for large quanti-

ties of sticks. This solution enabled sticks to be sent through a hose using a turbo blower (see Figure 8). The cyclone classifier received sticks blown by air flow, and transported them to the dispensing unit. Due to the weight of the dispensing unit (30 kg), it was hung on a rail to allow smooth operation by users. This limited its use to factory environments. We used the blower system in construction of the pavilion as a case study (Section 6) but in indoor use only because a gantry was required for the dispensing unit. This limited the available sites where we could operate the system.

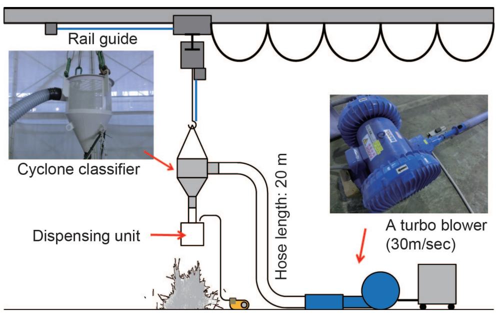

Figure 8: *Overview of the blower system.*

5 Guidance System

This section describes the guidance system, which used projection mapping. Its workflow was developed based on earlier works mentioned in Section 1 [Skeels and Rehg 2007; Rivers et al. 2012a] (Figure 9). The system captured the current work using a depth camera, compared the scanned geometry with the target shape, and then projected the guiding information based on an evaluation. Our contributions here were real time tracking and feedback using a depth camera, as well as operation workflow on an architectural scale. The workflow included a calibration procedure that supports relocation of the camera-projector system, thus allowing the guiding system to cover large objects.

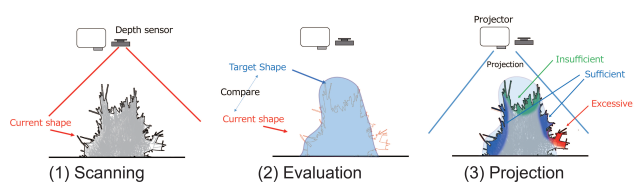

Figure 9: *Workflow of the guidance system.*

5.1 Hardware Setup

We set a projector-camera system on a 3.5 meter-high scaffold. A short throw projector, BenQ MX823ST, was selected for its wide projection area (approximately 4.0 m by 5.5 m at 3.3 m height). We used KINECT ver. 2 for the depth camera at a resolution of 512×424 at 30 fps. The Kinect2 was easy to use and also capable of outdoor use due to the time of flight (TOF) measurement mechanism.

5.2 User Interface

The captured current work and a target model are represented by voxels. The system evaluates each voxel, determined whether the current shape matched the target model, and then returned differences by displaying the evaluation results on each voxel. There are three types of evaluation results, as indicated in Figure 9:
(1) Insufficient: The detected voxel matched the target shape but requires additional printing. The color gradient (from green to blue) indicated how close the shape is to the desired shape. (2) Sufficient: The detected voxel matched the target shape. (3) Excessive: The detected voxel was outside the target shape. Results are displayed as 3D volumetric models and are also projected onto the current shape (Figure 10).

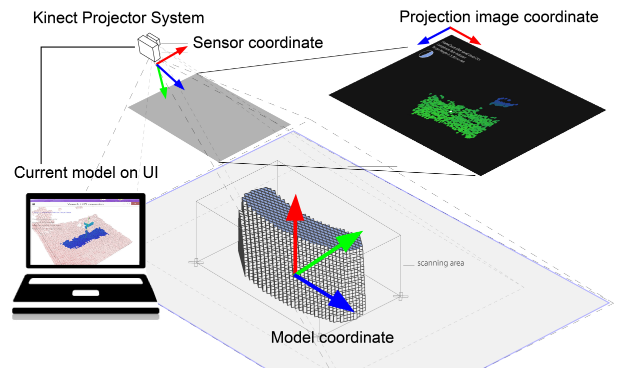

Figure 10: *UI and coordinate systems: Viewer UI on the left, projected image on the right. The model coordinate is in the bottom-center of the target model.*

5.3 Calibration

The guidance system requires a 3D coordinate system to represent the position and orientation of the target model. The coordinate system is also the basis of the evaluation process. In cases where the projector-camera system does not cover the entire target model, the system needs to be moved accordingly. For this reason, we developed a simple calibration procedure by defining three coordinate systems: a model world, a camera world, and a projector world. The model world is a 3D based coordinate system wherein the origin is defined on the bottom-center of the target model's bounding box (Figure 10). The camera world is a 3D coordinate system wherein the origin point and orientation are pre-determined via the depth camera. The projector world is a 2D coordinate system that illustrates the projection image. Calibration correlates (1) the model world and camera world, and (2) the model world and projector world.

Whenever the guidance system is set in a new position, a set of coordinates must be calibrated within the model world, camera world, and projector world (the obtained coordinates are referred to as a "set of coordinates"). To acquire these coordinates, we used physical markers whose positions had already been specified within the model world. In one example, 4 markers were placed on-site arbitrarily. Additional markers were set on a bar if height calibration was crucial. By clicking each marker on both a depth map and a projected image, the calibration process collected the clicked coordinates in the camera and projector worlds with preset marker positions (Figure 11). After collecting several sets of coordinates, we acquired a perspective projection matrix with the least-square method [Tsai 1987].

6 Case Study

To validate the feasibility of the proposed method and to clarify issues for real application, we designed and constructed a pavilion which was exhibited on a university campus for 12 days. The design of the pavilion was not determined in the pursuit of practical

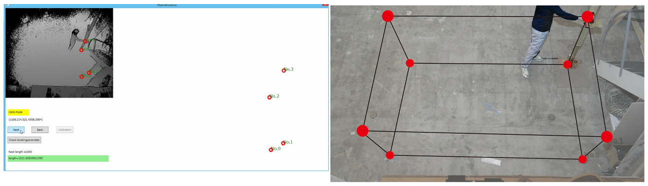

Figure 11: *Left: Calibration UI with a depth-map on the left and a projector world on the right. Right: Placement of a physical marker on a bar.*

architecture but instead aimed to test the developed methods, particularly in terms of free-form printing and on-site construction. Due to the daylight issue for operating a projector and the tight construction schedule, we split the pavilion into panels that were printed in controlled indoor environments. We then assembled them at the site. The pavilion was constructed over 20 days, which included placement of small scaffoldings, creation of a foundation, and water proof coat spraying. One million chopsticks were used to create the structure. Visitors were attracted to the exhibition from a distance, but expressed surprise upon discovery that the pavilion was made of chopsticks.

6.1 Geometry Design

The geometry was inspired by curves drawn by a harmonograph which are consisted of two damping pendulums. Simulating the path of a harmonograph and gradually elevating its height, we created a cylindrical, double-curved surface. Given the material specifications described in Section 3, we did a structural analysis using a Finite Element Method (FEM); beam elements were used to inform structurally crucial areas, which largely consisted largely of areas where steep overhangs appeared (left in Figure 12). Although the structure was self-supporting, stainless steel wire cables were embedded in case of unexpected loads (such as strong winds). The cables were placed every 500 mm, both horizontally and vertically. The vertical cables were connected to weights placed at the foundation, which weighing 3 tons in total. The entrance opening was also reinforced. Furthermore, the thickness of the surface was tapered from 800 mm at the bottom to 200 mm at the top to stabilize the structure.

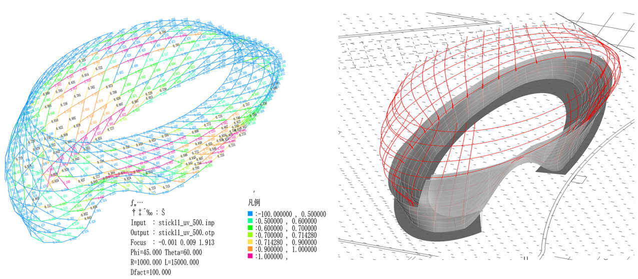

Figure 12: *Structural analysis and reinforcement: FEM analysis results using beam elements (left), and fail-safe wire cables (right).*

6.2 Panelized Construction

In addition to addressing the daylight issue described earlier in this section, panelized construction also proved effective for minimizing the required printing operations outdoors, where we encountered rain and other weather-related difficulties. The first meter of the pavilion was attached to weights, making the form impractical to carry. For this reason, the first meter (indicated in red in the inset figure) was printed on-site with multiple guidance systems. For the remaining portions of the pavilion (which was 3.8 m in height), the geometry was divided into 35 panels that were printed indoors (indicated in blue in the inset figure). Using the aforementioned blower system, we printed 10 panels, and we printed 25 panels with the handheld dispensers. When modeling the panels, we created gaps between panels and filled them in on-site, much the way mortar is used in brickwork.

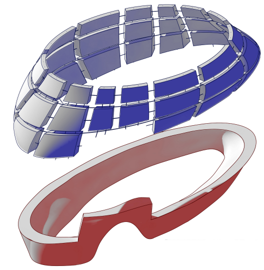

6.3 On-site Calibration

As previously described, we printed the first vertical meter of sticks on-site using the developed guidance system. To operate the system on-site, a local model world must be set in relation to the entire target model. To calibrate each local model world, we used physical markers distributed on-site in pre-determined locations (Figure 13). Once the local world had been calibrated, printing operations were the same as those described in Section 5. We repeated the process after finishing each target. To place panels on-site after constructing the first meter in height, we modified the guidance system to allow horizontal projection, thus enabling the system to check the alignment of the panels.

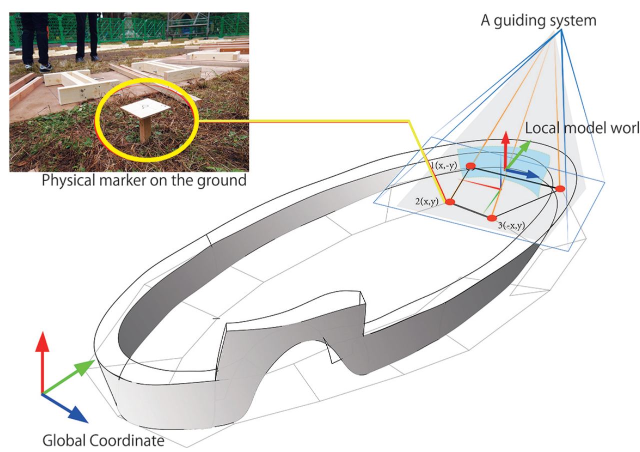

Figure 13: *On-site calibration with physical markers.*

6.4 Lessons Learned

In many cases, workers needed to check the growth direction of a target shape to adjust the stick-dropping angle. It was impossible, however, to determine the growth direction purely through the use of the guidance system because the system only indicated only whether the current work matched the target model or if it required additional sticks. To address this issue, a board placed at an arbitrary height could be used to check the the guidance system results (on the board rather than on the work in progress) (Figure 14). This works as a lens that shows invisible volume in mid-air. By moving the board up and down, workers were able to intuitively understand the growth direction of the current work.

Unfortunately, the guidance system was used in few areas during on-site construction for a number of reasons. Due to daylight, there were limited periods of time during which the projector could be operated. Although it was possible to operate the system at night, this was avoided for safety reasons. Another issue encountered was related to the calibration space. The space—defined by fixed physical markers—was often blocked by other objects (such as small scaffolding) on-site. The entire site could be covered by a large scaffolding to block daylight and rain, but it was cancelled due to financial constraints.

Due to the limited operation of the guidance system, some areas or panels did not match the targeted shapes. In these cases, panels were aligned using conventional drawings and measurements. This process, however, created tedious work and necessitated repetitive measurements over uneven surfaces, followed by re-positioning of the panels. Small errors were accumulated from the bottom layers, resulting in an unaligned top ring (see Figure 1(iv)). In crucial areas of the structure or sections difficult to print (such as the openings), printing operations were physically guided using nets or boards as formworks.

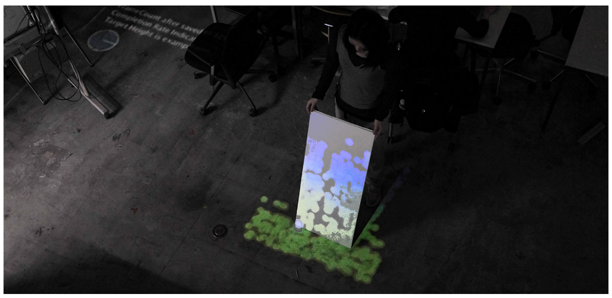

Figure 14: *A user checking the growth direction of a target model.*

7 Limitations and Future Work

We proposed a new computer-assisted digital fabrication method for architecture-scale objects. Our proposal consists of three technical developments: use of a chopstickglue composite as a printing material, a stick dispenser as a printing tool, and a guiding system that indicates printing locations to workers. We explored the geometric and mechanical properties of the created porous structure (which consists of chopsticks and glue) through several material tests and a comparison of constitutive factors with several other materials. We presented the mechanism of the stick dispenser and its operation method and demonstrated the guiding system (which uses a projectorcamera system), to scan the current work and project the guidance onto the work with a simple color code. The pavilion was designed and constructed with our proposed method, and the project provided further insights and findings via the construction process.

Compared to conventional building materials (such as timber and steel), the chopstickglue composite without reinforcement is relatively weak as a structural building material. Stronger binders, such as hot-melt glue, can improve strength and provide higher resistance against weathering. If printing with threads or nets, the composite material's tensile strength can be reinforced. These additions can be applied locally after printing to reinforce structurally critical points. Due to the roughness of the material, it is difficult to achieve geometries requiring high degrees of precision (such as flat surfaces). For such precise work, physical jigs or formworks are effective for guiding approximate outlines; however, the resulting surface loses the “spiked” material texture. In these cases, flexible nets can serve as formworks while also working to maintain the material's texture, which was examined in the opening area of the pavilion.

An analysis of the material indicated the stickglue composite is anisotropic, but our material tests were limited to one direction. In sample tests, the material suggested resistance to bending forces rather than axial loads; however, more samples are necessary to validate this tendency. Aggregation behaviors were distinguished into two modes—jammed and stratified—but this may be an oversimplification. In the future, we plan to find a way to model the complex behavior of the dropped stickglue composite and incorporate it into a design tool.

The guidance system cannot be operated in daylight. Implementation of a temporary enclosure for use throughout the construction period is highly recommended to block all sunlight and rain. Intelligent power tools with built-in interfaces and sensors could also provide workers with information regarding construction processes [Zoran et al. 2013; Rivers et al. 2012b]. Our handheld dispenser could be developed as an intelligent power tool, but sharing information among multiple tools would be a challenge for large-scale construction. Additional work would be required to set up a motion-tracking system on-site. AR devices such as head-mounted displays (HMDs) could serve as interfaces, but would require calibration on each device. The proposed projector-camera guidance system can be prepared with a simple calibration process, and would also allow for intuitive information-sharing among workers.

Adaptive modification of the target shape could be useful in cases where the current work is significantly different from the target shape. Zoran et al. [2013] explored method with dynamic modeling that compensates for errors during fabrication. This development could potentially be used to share model updates among workers cooperating on-site.

8 Acknowledgments

We would like to thank the team from Shimiz Corp. : H. Umeyama, T. Satoh, H. Ogura, K. Tanno, M. Indo, K. Takeuchi. The pavilion could not be built without the supports from the lab staffs and students: S. Sugita, TK. Kiuchi, TH. Kiuchi, K. Clement, A.Rod, M. Xu, F. Osman, Q. Jin, O. Saraya, B. Berwick, Y. Xiong, J.Vranovsky, G. Judhinaputra, P. Virutamawongse, S. Aaron, R. Shatarova, R. Sam, Y. Xu, D. Lopez, H. Habib, A. Crusius, M. Mori, A. Karlsson, Y. Lu, J. Lai. We thank M.Nakamoto and his colleagues for providing leftover chopsticks almost for free. Finally, we thank A. Ivelich for her continuous English collection.

References

AZUMA, R. T., ET AL. 1997. A survey of augmented reality. *Presence 6*, 4, 355–385.

BENKO, H., JOTA, R., AND WILSON, A. 2012. Miragetable: freehand interaction on a projected augmented reality tabletop. In *Proc. of CHI '12*, 199–208.

BENKO, H., WILSON, A. D., AND ZANNIER, F. 2014. Dyadic projected spatial augmented reality. In *Proc. of UIST '14*, 645–655.

BICKEL, B., BÄCHER, M., OTADUY, M. A., MATUSIK, W., PFISTER, H., AND GROSS, M. 2009. Capture and modeling of non-linear heterogeneous soft tissue. 89.

BICKEL, B., BÄCHER, M., OTADUY, M. A., LEE, H. R., PFISTER, H., GROSS, M., AND MATUSIK, W. 2010. Design and fabrication of materials with desired deformation behavior. *ACM Trans. Graph 29*, 4, 63.

BOCK, T. 2007. Construction robotics. *Autonomous Robots 22*, 3, 201–209.

BOGUE, R. 2013. 3d printing: the dawn of a new era in manufacturing? *Assembly Automation 33*, 4, 307–311.

CALÌ, J., CALIAN, D. A., AMATI, C., KLEINBERGER, R., STEED, A., KAUTZ, J., AND WEYRICH, T. 2012. 3d-printing of non-assembly, articulated models. *ACM Trans. Graph 31*, 6, 130.

CESARETTI, G., DINI, E., DE KESTELIER, X., COLLA, V., AND PAMBAGUIAN, L. 2014. Building components for an outpost on the lunar soil by means of a novel 3d printing technology. *Acta Astronautica 93*, 430–450.

DE GOES, F., ALLIEZ, P., OWHADI, H., DESBRUN, M., ET AL. 2013. On the equilibrium of simplicial masonry structures. *ACM Trans. Graph 32*, 4.

DEUSS, M., PANOZZO, D., WHITING, E., LIU, Y., BLOCK, P., SOKRINE-HORNUNG, O., AND PAULY, M. 2014. Assembling self-supporting structures. *ACM Trans. Graph 33*.

DIERICHS, K., AND MENGES, A. 2010. Material computation in architectural aggregate systems. *In Proc. of ACADIA*, 372–378.

DORSEY, J., AND MCMILLAN, L. 1998. Computer graphics and architecture: state of the art and outlook for the future. *ACM SIGGRAPH Comput. Graph. 32*, 1, 45–48.

FAIRS, M., 2002. Arne quinze at burning man - dezeen. http://www.dezeen.com/2007/05/01/arne-quinze-at-burning-man/.

FLAGG, M., AND REHG, J. M. 2006. Projector-guided painting. In *Proc. of UIST '06*, 235–244.

FREARSON, A., 2014. Chinese company 3d prints 10 buildings in a day using construction waste. http://www.dezeen.com/2014/04/24/chinese-company-3d-prints-buildings-construction-waste/.

JONES, B., SODHI, R., MURDOCK, M., MEHRA, R., BENKO, H., WILSON, A., OFEK, E., MACINTYRE, B., RAGHUVANSHI, N., AND SHAPIRA, L. 2014. Roomalive: magical experiences enabled by scalable, adaptive projector-camera units. In *Proc. of UIST '14*, 637–644.

JU, W., BONANNI, L., FLETCHER, R., HURWITZ, R., JUDD, T., POST, R., REYNOLDS, M., AND YOON, J. 2002. Origami desk: integrating technological innovation and human-centric design. In *Proc. of DIS '02*, 399–405.

KHOSHNEVIS, B. 2004. Automated construction by contour crafting? related robotics and information technologies. *Automation in construction 13*, 1, 5–19.

LOVATT, A., AND SHERCLIFF, H., 2002. Material selection and processing. http://www-materials.eng.cam.ac.uk/mpsite/default.html.

LU, L., SHARF, A., ZHAO, H., WEI, Y., FAN, Q., CHEN, X., SAVOYE, Y., TU, C., COHEN-OR, D., AND CHEN, B. 2014. Build-to-last: Strength to weight 3d printed objects. *ACM Trans. Graph 33*, 4, 97.

PAI, D. K., DOEL, K. V. D., JAMES, D. L., LANG, J., LLOYD, J. E., RICHMOND, J. L., AND YAU, S. H. 2001. Scanning physical interaction behavior of 3d objects. In *Proc. of SIGGRAPH '01*, 87–96.

PANOZZO, D., BLOCK, P., AND SORKINE-HORNUNG, O. 2013. Designing unreinforced masonry models. *ACM Trans. Graph 32*, 4, 91.

PEREIRA, T., RUSINKIEWICZ, S., AND MATUSIK, W. 2014. Computational light routing: 3d printed optical fibers for sensing and display. *ACM Trans. Graph 33*, 3, 24.

PIPER, B., RATTI, C., AND ISHII, H. 2002. Illuminating clay: a 3-d tangible interface for landscape analysis. In *Proc. of CHI '02*, 355–362.

PRÉVOST, R., WHITING, E., LEFEBVRE, S., AND SORKINE-HORNUNG, O. 2013. Make it stand: balancing shapes for 3d fabrication. *ACM Trans. Graph 32*, 4, 81.

RASKAR, R., WELCH, G., AND FUCHS, H. 1998. Seamless projection overlaps using image warping and intensity blending. Fourth International Conference on Virtual Systems and Multimedia, Gifu, Japan.

RIVERS, A., ADAMS, A., AND DURAND, F. 2012. Sculpting by numbers. *ACM Trans. Graph 31*, 6, 157.

RIVERS, A., MOYER, I. E., AND DURAND, F. 2012. Position-correcting tools for 2d digital fabrication. *ACM Trans. Graph 31*, 4, 88.

SKEELS, C., AND REHG, J. M. 2007. Shapeshift: A projector-guided sculpture system. In *Proc. of UIST '07 poster session*.

SODHI, R., BENKO, H., AND WILSON, A. 2012. Lightguide: projected visualizations for hand movement guidance. In *Proc. of CHI '12*, 179–188.

SONG, P., FU, C.-W., GOSWAMI, P., ZHENG, J., MITRA, N. J., AND COHEN-OR, D. 2013. Reciprocal frame structures made easy. *ACM Trans. Graph 32*, 4, 94.

TSAI, R. Y. 1987. A versatile camera calibration technique for high-accuracy 3d machine vision metrology using off-the-shelf tv cameras and lenses. *Robotics and Automation 3*, 4, 323–344.

VOUGA, E., HÖBINGER, M., WALLNER, J., AND POTTMANN, H. 2012. Design of self-supporting surfaces. *ACM Trans. Graph 31*, 4, 87.

WHITING, E., SHIN, H., WANG, R., OCHSENDORF, J., AND DURAND, F. 2012. Structural optimization of 3d masonry buildings. *ACM Trans. Graph 31*, 6, 159.

WILSON, A., BENKO, H., IZADI, S., AND HILLIGES, O. 2012. Steerable augmented reality with the beamatron. In *Proc. of UIST '12*, 413–422.

ZHOU, Q., PANETTA, J., AND ZORIN, D. 2013. Worst-case structural analysis. *ACM Trans. Graph 32*, 4, 137.

ZORAN, A., SHILKROT, R., AND PARADISO, J. 2013. Human-computer interaction for hybrid carving. In *Proc. of UIST '13*, 433–440.